

Journal of Geophysical Research Letters
Supporting Information for

InSAR observations of strain accumulation and fault creep along the Chaman Fault system, Pakistan and Afghanistan

H. Fattahi¹, F. Amelung²

¹Seismological Laboratory, California Institute of Technology, Pasadena, California,
USA.

²Rosenstiel School of Marine and Atmospheric Science, University of Miami, Miami,
FL, USA, ²Department of Earth and Planetary Science, University of California,
Berkeley, Berkeley, CA, USA

Content of this File

Figures S1 to S8

Table S1

Section S1. Transects across southern Chaman Fault system and Makran Ranges

Section S2. Slip deficit on the creeping section

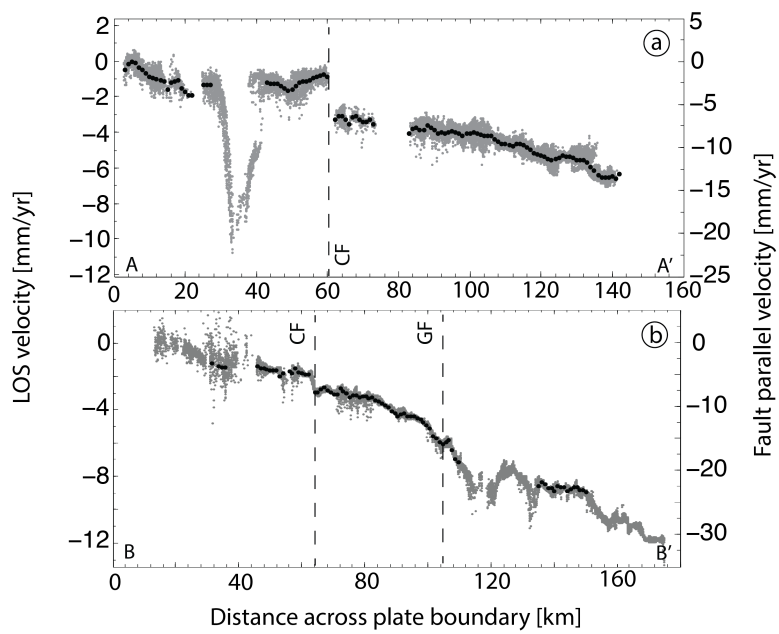


Figure S1: same as Figure 2a,b, but the black dots show the sampled data used for modeling.

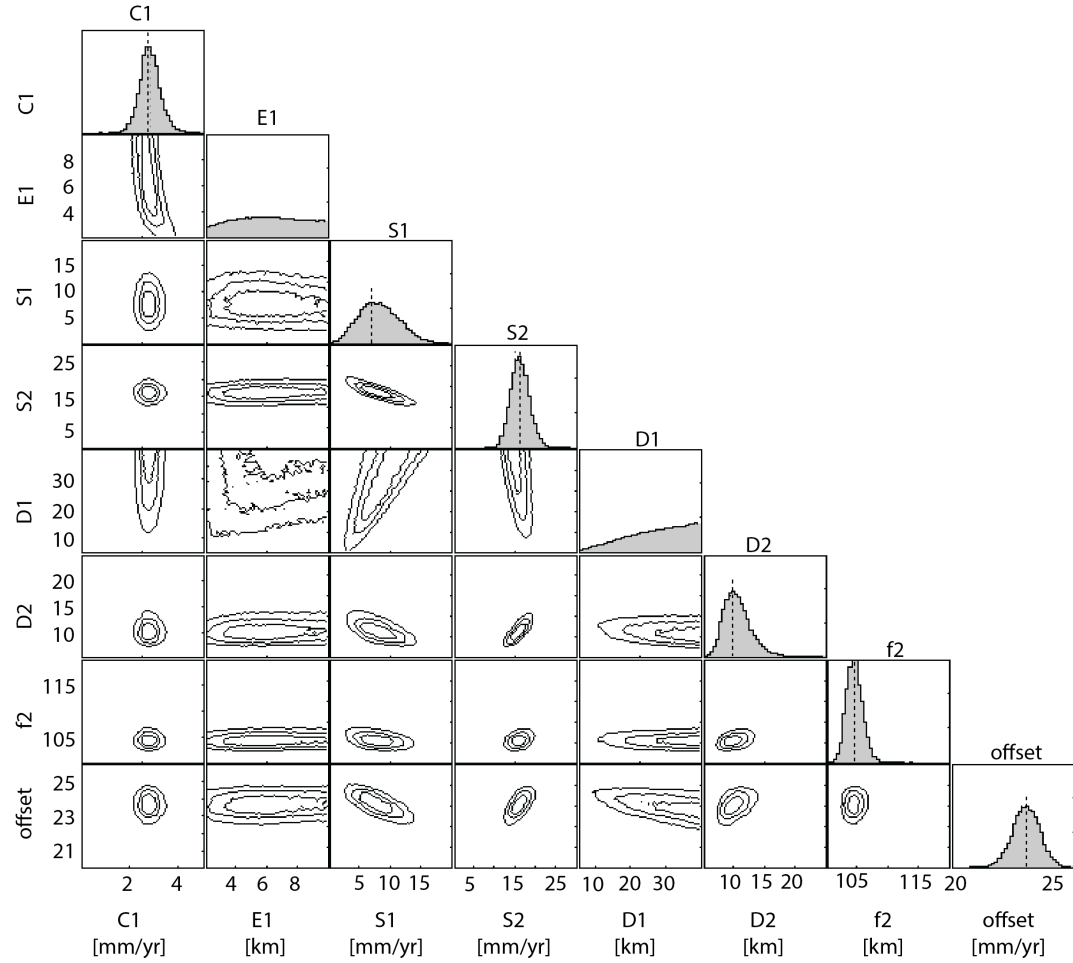


Figure S2: Marginal posterior density distribution of model parameters and the contours of the joint distributions obtained for transect BB' in Figure 2b. C1: creep rate of Chaman fault, E1: creep extent of Chaman fault, S1: slip rate of Chaman fault, S2: slip rate of Ghazaband fault, D1: locking depth of Chaman fault, D2: locking depth of Ghazaband fault, f2: location of Ghazaband fault, offset: a constant offset. Gibbs sampling with 200000 sweeps at the critical Temperature of 1. Dashed vertical line denotes the mode of the distribution.

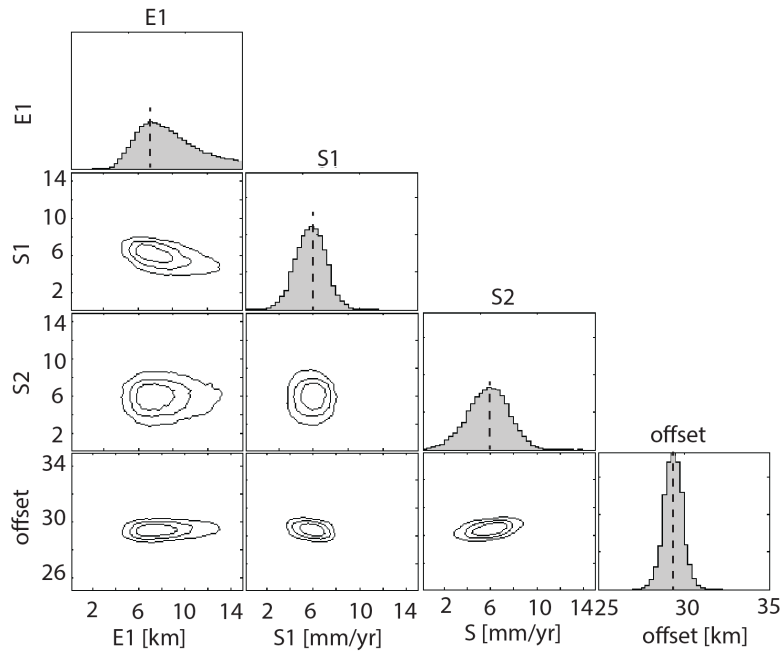


Figure S3: Marginal posterior density distribution of model parameters and the contours of the joint distributions obtained from Gibbs sampling with 200000 sweeps at a critical temperature of 1 for transect AA' in Figure 2a. E1: creep extent of Chaman fault, S1: slip rate of Chaman fault, S2: slip rate of the arbitrary fault at km 125, offset: a constant offset.

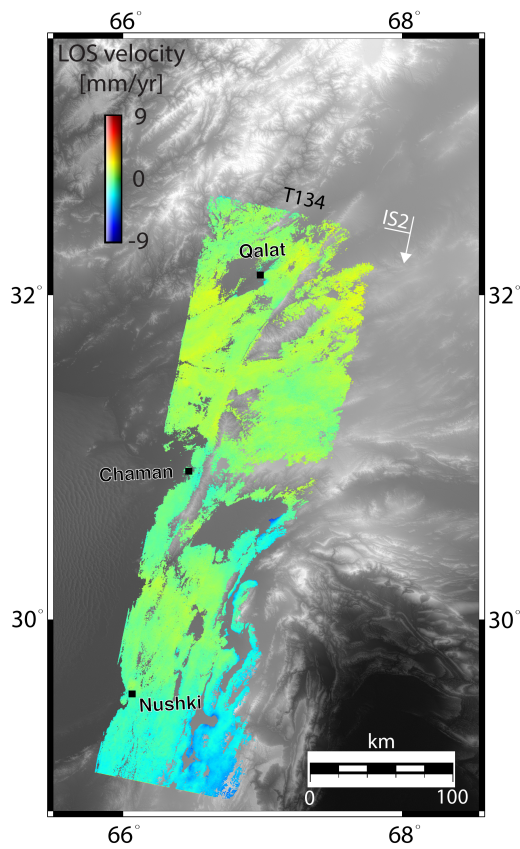


Figure S4: LOS velocity field for the Central Chaman fault system from descending track 134.

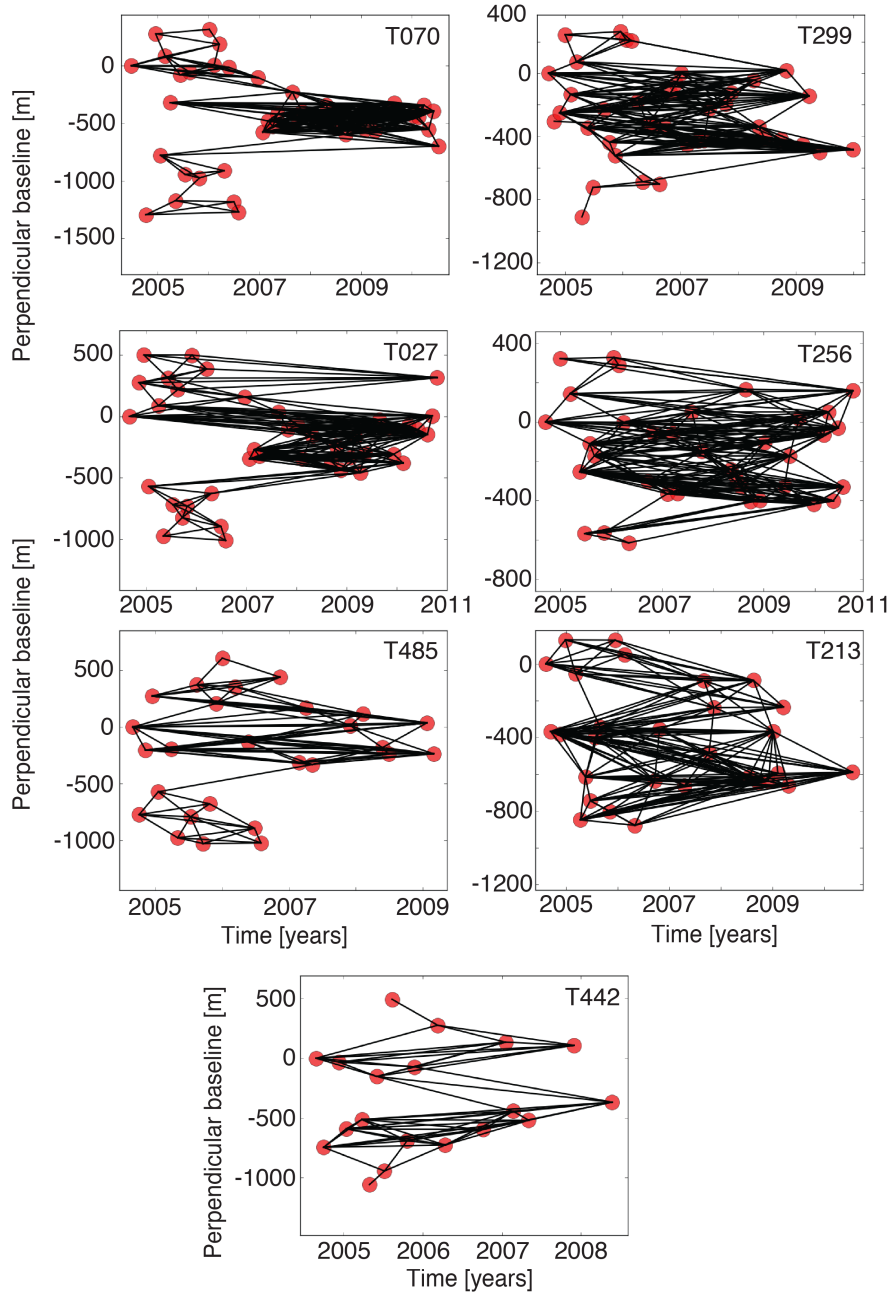


Figure S5: Network of interferograms for 7 ascending tracks used to produce the velocity field in Figure 1.b.

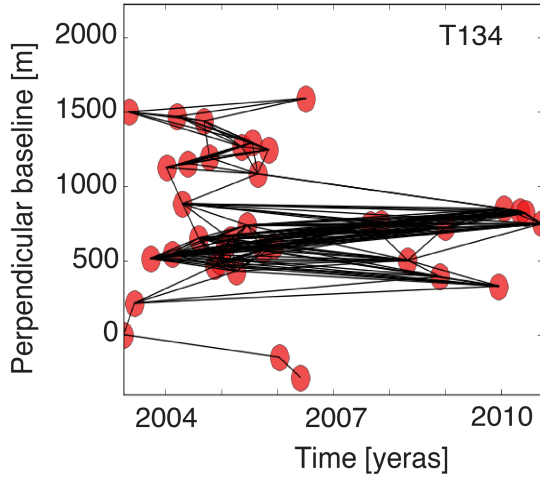


Figure S6: The network of interferograms for descending track 134 used to generate the InSAR velocity field in Figure S4.

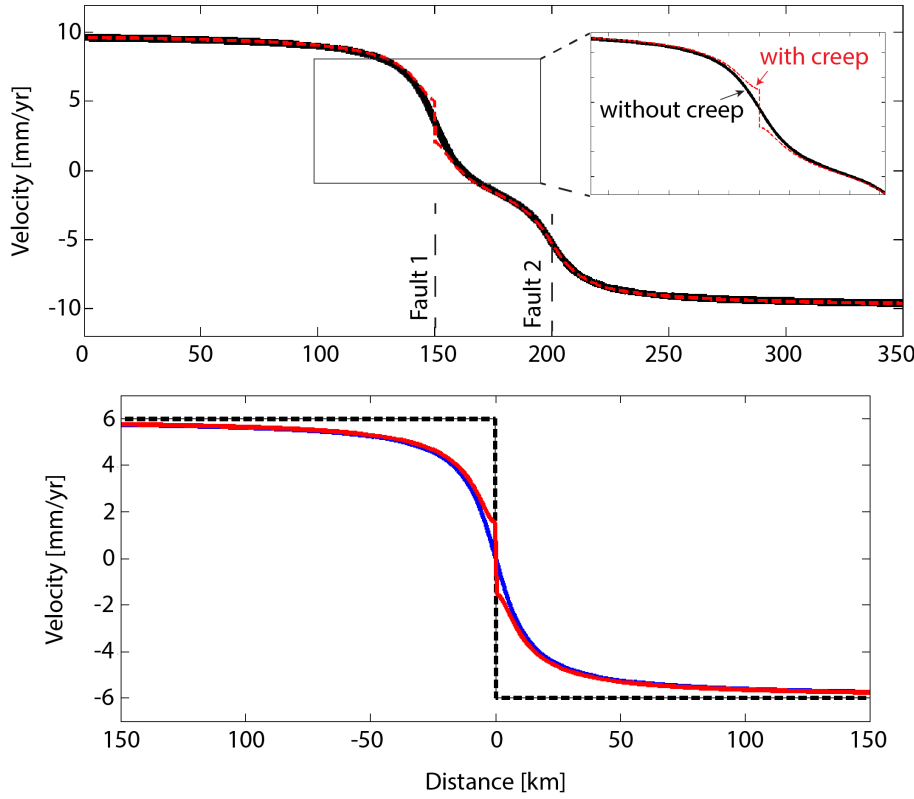


Figure S7: Example for the fault parallel velocity due to a strain accumulation on a) two faults with slip rates of 12 and 8 mm/yr and locking depth of 10 km without fault creep at shallow depth (solid black line) and with shallow creep of 3 mm/yr from surface to 3 km depth of Fault 1 (red dashed line). The total fault parallel velocity across the faults is 20 mm/yr, b) one vertical strike-slip fault with a slip rate of 12 mm/yr and locking depth of 10 km (blue solid line); same but surface fault creep at a rate of 3 mm/yr to 3 km depth (red line); and for fault creep through the entire seismogenic depth (black dashed line).

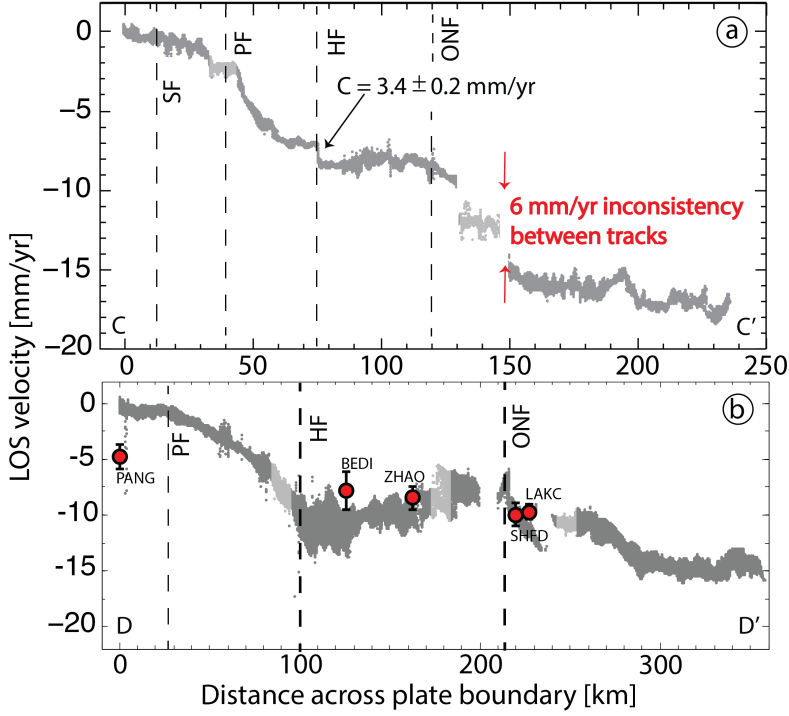


Figure S8: a,b Same as Figure 2 but for profiles CC' and DD'. a is perpendicular to the Hoshab fault (oriented N69W) and b (oriented N65W) follows the GPS profile of Szeliga et al. [2012]. The uncertainties over the transect lengths (225 and 350 km) are 3.6 and 4 mm/yr LOS. Red circles in (b): GPS observations projected into LOS direction with 2 sigma uncertainty from Szeliga et al [2012].

Table S1: Same as Table 1 but for three different models for profile AA'. A) same as in main text but with a locking depth of 10 km for the two hypothetical faults, B) same as in main text but using only one arbitrary fault, C) same as model B but with locking depths of 10 km.

Profile	Fault	S [mm/yr]	D [km]	C[mm/yr]	E[km]	f[k]
AA'	Chaman	6.6 ± 1.2	15*	5*	7.8 ± 2.4	60*
	Arbitrary	7.7 ± 1.3		0*	0*	125*
AA'	Chaman	5.7 ± 1.3	15*	5*	8.5 ± 2.5	60*
	Arbitrary1	2.7 ± 1.7		0*	0*	105*
	Arbitrary2	5.7 ± 1.8		0*	0 *	125*
AA'	Chaman	5.4 ± 1.2	10*	5*	6.9 ± 2.3	60*
	Arbitrary1	3.1 ± 1.3		0*	0*	105*
	Arbitrary2	4.2 ± 1.4		0*	0 *	125*

Section S1. transects across southern Chaman Fault system and Makran Ranges

Transect CC' across the southern Chaman fault system shows \sim 8 mm/yr relative LOS velocity over 140 km in the easternmost Makran (Figure S8a), consisting of \sim 7 mm/yr across the Panjgur Fault and \sim 1 mm/yr discontinuity across the Hoshab Fault, corresponding to a surface creep rate of 3.4 ± 0.2 mm/yr (local fault strike of 21°), just northeast of the rupture of the 2013 $M_w7.7$ earthquake. The transect shows another 2 mm/yr of relative LOS velocity east of 160 km. However, an inconsistency between two adjacent tracks prevents us from estimating the rate of strain accumulation. Transect DD' (Figure S8b) coincides with the GPS stations of *Szeliga et al.* [2012] shows 15 mm/yr relative LOS velocity over its length, 10 mm/yr of which occurs over the Makran faults (between 0 km and 150 km distance) and 5 mm/yr over the southern Chaman Fault system (between 150 and 350 km). We don't interpret this observation in terms of strain accumulation rate because of the uncertainty (3.5 mm/yr over 200 km) and because our measurements are not sensitive to motion along the north-south trending Ornach Nal Fault. The transect is overall consistent with the GPS horizontal velocities projected in LOS direction of *Szeliga et al.* [2012], except for the station PANG. The discrepancy may represent vertical deformation, which is not captured by GPS. However, it falls within the InSAR uncertainty, which is in this area anomalously high (\sim 4 mm/yr over 100 km; see Figure 6b of *Fattah and Amelung*, [2015]).

Section S2. Slip deficit on the creeping section

For the creeping segment the tectonic loading rate corresponds to 1 m of slip accumulated over the 124 years since the 1892 earthquake. About one third of the slip has been accommodated seismically (the summed moment of the three earthquakes corresponds to

an averaged slip of 0.37 m for 340 km fault length and locking depth of 10.6 km). As our data do not have the resolution to infer the coupling coefficient, we make the rough estimate that one quarter of the slip is accommodated aseismically (inferred from the observation that the surface creep is about half the loading rate and assuming a creep extent of half of the locking depth). This leaves 0.38 m of potential slip available for the next rupture. Here we have assumed that creep has been constant over the time period considered and we have ignored aftershocks and afterslip.